Impact of electron density profile on core impurity behaviour in NBI-heated LHD plasmas

N. Tamura[1], C. Suzuki[2,3], M. Goto[2,3], Y. Kawamoto[2,3], R. T. Ishikawa[2,3], T. Oishi[4], M. Yoshinuma[2], K. Ida[2], K. Mukai[2,3], K. Tanaka[2,5], T. Tokuzawa[2,3], H. Funaba[2], I. Yamada[2,3]

[1]Max-Planck Institute for Plasma Physics, Greifswald, Germany, [2]National Institute for Fusion Science, Toki, Japan, [3]The Graduate University for Advanced Studies (SOKENDAI), Toki, Japan, [4]Tohoku University, Sendai, Japan, [5]Kyushu University, Fukuoka, Japan

Introduction Magnetically confined high-temperature plasmas are strongly influenced by the electron density, n_e, profile, which is one of the key parameters determining overall plasma performance. Plasmas with a peaked density profile generally exhibit improved confinement and enhanced performance, not only in tokamaks [e.g., 1] but also in helical devices [e.g., 2]. However, a peaked density profile is not always beneficial. From the viewpoint of neoclassical transport, it can promote impurity accumulation in the plasma core, which may eventually lead to plasma degradation or even radiative collapse [e.g., 3]. Therefore, it is important to investigate how the shape of the n_e profile affects the behaviour of core impurities. We have studied the impact of n_e profile shape on the behaivour of core impurities by using the Fe-Tracer-Encapsulated Solid Pellet (TESPEL) [4] in Large Helical Device (LHD).

Experimental setup In this study, the experiments have been carried out in the LHD standard magnetic configuration, R_{ax} = 3.6 m and B_t = +2.75 T. To control the n_e profile, a tangential NBI was selected as the baseline heating method for flat density profiles, while a perpendicular NBI was selected for peaked density profiles. In addition to the baseline heating, a modulated perpendicular NBI was applied as a probe beam for charge-exchange spectroscopy, which measures the spatio-temporal evolution of the ion temperature, radial electric field, and so on. A Fe impurity, the amount (N_{Fe} ~ 7.1 x 10^{18} particles) of which was the same in both profile cases, was injected into the plasma using a TESPEL method. To vary the deposition location of the Fe impurity, the smaller (600 um O.D. with a shell thickness of 80 um) and larger (900 um O.D. with a shell thickness of ~300 um)) TESPELs were used. The temporal behaviours of the line emissions from highly ionized Fe impurity were tracked with EUV/VUV spectrometers, SOXMOS (temporal resolution: 50 ms) [5] and EUVShort (temporal resolution: 5 ms) [6]. The spatio-temporal behaviour of the line emissions from highly ionized Fe impurity was observed with a space-resolved EUV spectrometer, EUVShort2 (temporal resolution: 100 ms) [7]. The spatio-temporal evolution of n_e and electron temperature, T_e, was measured with the Thomson Scattering diagnostic [8]. In this experiment, to minimize the effect of magnetic island on the impact of the TESPEL injection on the plasma profile, a resonant magnetic perturbation was applied to cancel a m/n = 1/1 natural magnetic island.

Experimental results and discussions Figure 1 shows the impact of TESPELs with different sizes on plasmas with a peaked n_e profile. By using only perpendicular NBIs, the n_e profile becomes peaked. When the smaller TESPEL was injected (estimated tracer deposition location: r_{eff}/a_{99} ~ 0.8), the n_e and T_e profiles did not respond significantly to the TESPEL injection. In contrast, when the larger TESPEL was injected (estimated tracer deposition location: r_{eff}/a_{99} ~ 0.45-0.6), both the n_e and T_e profiles exhibited a pronounced response to the TESPEL injection. The T_e profile gradually decreased from around r_{eff}/a_{99} = 0.8 toward the plasma centre and became nearly flat at t = 4.467 s. After the profile had flattened, the central T_e decreased further and remained in this state for about 0.1 s. Subsequently, the reduced-temperature region began to recover globally. However, the original profile was not restored by t = 5.3 s, although the heating conditions remained unchanged throughout this period. On the other hand, the n_e profile

increased mainly in the region penetrated by the TESPEL until t = 4.467 s, when the T_e profile became flat, while the plasma core remained almost unchanged. This result suggests that the decrease in the central T_e was not an adiabatic response associated with an increase in the central n_e. Thereafter, the n_e in the peripheral region remained nearly constant, whereas the n_e in the plasma core increased. The increase in n_e following the injection of the larger TESPEL was greater than that attributable to perpendicular NBI as the baseline heating source. Figure 2 shows the impact of TESPELs with different sizes on plasmas with a flatter n_e profile. It should be noted that the n_e profile was not completely flat because of the influence of the modulated perpendicular NBI. For the smaller TESPEL, the impact on the plasma was similarly limited to that observed in the peaked n_e profile case, and no significant changes were observed. For the larger TESPEL, the T_e decreased in the region penetrated by the TESPEL. However, unlike in the peaked n_e profile case, the reduction in T_e did not propagate toward the plasma core. These results demonstrate that, despite the injection of identical TESPELs, the plasma response can differ substantially depending on the plasma conditions. It should be noted that the target plasma with the flatter density profile had a central T_e about 0.4 keV higher than that of the peaked n_e profile plasma. Consequently, the TESPEL penetration depth was slightly shallower in the flatter n_e profile case than in the peaked n_e profile case. These observations indicate that the core plasma response to TESPEL injection is not determined solely by the injected impurity amount but is strongly governed by the impurity deposition location together with the background density and temperature profiles. Here, it is important to check the behaviours of impurities injected into each profile case. Figure 3 shows the behaviours of line emissions from highly ionized Fe impurity injected into the plasma with the peaked n_e profile. For the smaller TESPEL, the Fe line emissions gradually decreased with time, and then they go back finally to the pre-injection level (see Fig. 2(h) also in terms of profile). For the larger TESPEL, the emission lines from higher charge-state Fe ions, Fe XXII - XXIV, decreased below their pre-injection levels immediately after TESPEL injection and became nearly undetectable. At the same time, the emission lines from lower charge-state Fe

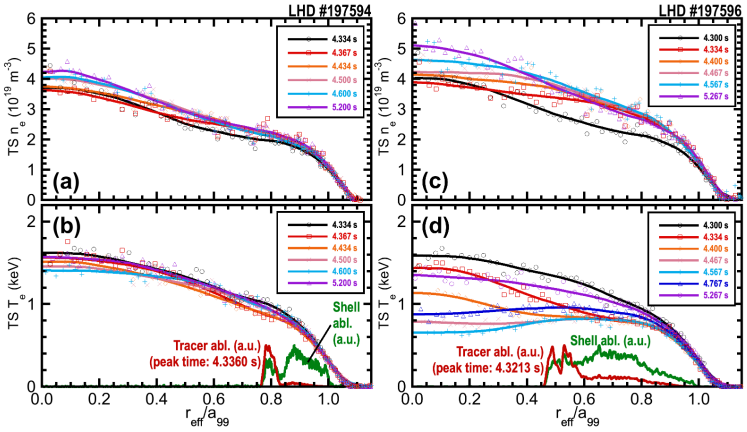

Fig. 1. Temporal evolutions of electron density, n_e, and temperature, T_e, profile just before (black) and after (red, blue, purple) the TESPEL injection for the plasmas with a peaked density profile: (a, b) for the smaller TESPEL case (LHD #197594) and (c, d) for the larger TESPEL case (LHD #197596). The radial profiles of ablation emissions from the TESPEL shell and tracers are also plotted in the frame of T_e profiles.

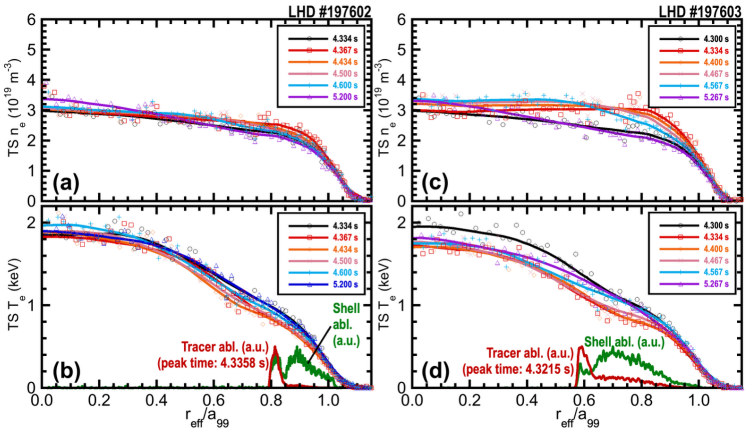

Fig. 2. Temporal evolutions of electron density, n_e, and temperature, T_e, profile just before (black) and after (red, blue, purple) the TESPEL injection for the plasmas with a flat density profile: (a, b) for the smaller TESPEL case (LHD #197602) and (c, d) for the larger TESPEL case (LHD #197603). The radial profiles of ablation emissions from the TESPEL shell and tracers are also plotted in the frame of T_e profiles.

ions, Fe XVII - XIX, increased significantly. During some periods, the increase was so large that the signals became saturated. Subsequently, as the T_e recovered, the Fe XVII - XIX emissions decreased, while the Fe XXII - XXIV emissions gradually increased. These results indicate that, for small TESPELs, the impurity accumulation predicted from the peaked density profile did not occur, and the injected Fe was almost completely expelled from the plasma. In contrast, for the larger TESPEL, Fe remained in the plasma for a relatively long period, while undergoing progressive changes in its ionization balance in response to the evolving T_e. Figure 4 shows the behaviours of line emissions from highly ionized Fe impurity injected into the plasma with the flat n_e profile. In this case, the line emissions from Fe ions exhibited similar behaviour for both the smaller and larger TESPELs. The Fe line emissions were dominated by the higher charge states, Fe XXII - XXIV, and remained at levels higher than those observed before the TESPEL injection (also see Fig. 4(h)). This observation indicates that impurity accumulation occurred in both cases. It should be noted, however, that the temporal evolution of the Fe XXIV emission a bit differed between the two cases. The peak appeared a bit earlier for the larger TESPEL than for the smaller TESPEL. This result suggests that the farther the impurities are deposited from the plasma core, the longer it takes for them to accumulate in the core region. Thus, the impurity behaviour observed here cannot be understood solely from the n_e profile shape; the deposition location must also be considered, as it affects both the retention or expulsion of Fe impurities and the timescale of their accumulation in the core.

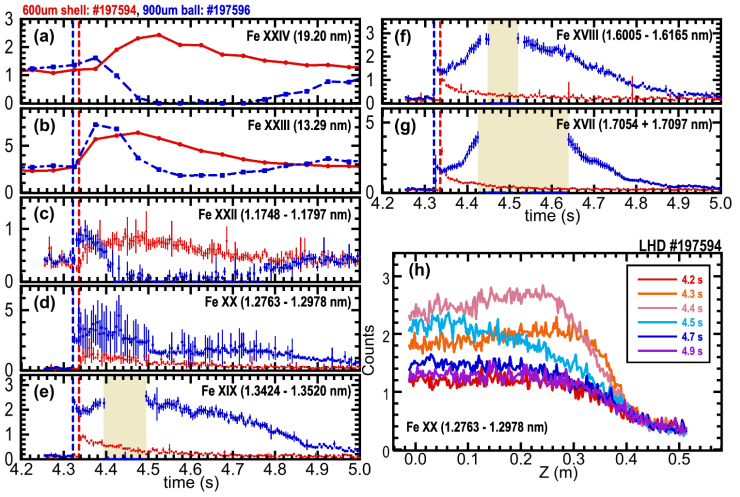

Fig. 3. Temporal evolutions of the line emissions from the highly ionized Fe impurity injected with the TESPEL into the plasmas with a peaked density profile; (a) Fe XXIV (19.20 nm), (b) Fe XXIII (13.29 nm), (c) Fe XXII (1.1748 – 1.1797 nm), (d) Fe XX (1.2763 – 1.2978 nm), (e) Fe XIX (1.3424 – 1.3520 nm), (f) Fe XVIII (1.6005 – 1.6165 nm), (g) Fe XVII (1.7054 + 1.7097 nm). The vertical dashed lines indicate the peak time of the TESPEL shell ablation for each case. The coloured-hatched regions indicate the region where the CCD counts are saturated. (h) Vertical profile evolution of the Fe XX emissions just before and after the injection of the smaller TESPEL.

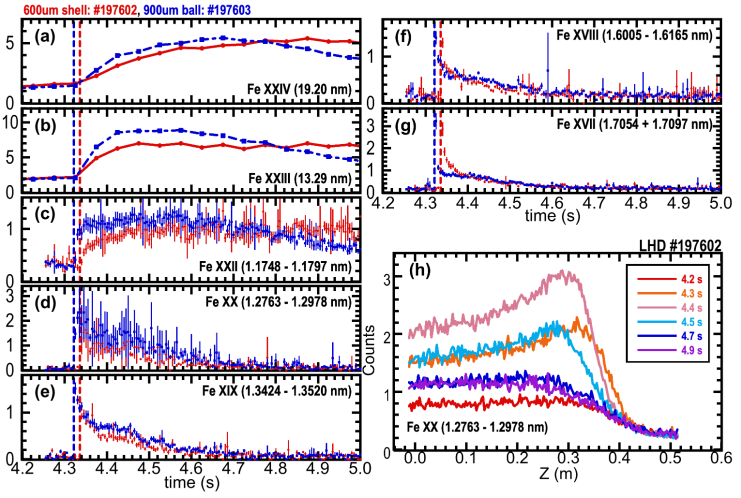

Fig. 4. Temporal evolutions of the line emissions from the highly ionized Fe impurity injected with the TESPEL into the plasmas with a flat density profile; (a) Fe XXIV (19.20 nm), (b) Fe XXIII (13.29 nm), (c) Fe XXII (1.1748 – 1.1797 nm), (d) Fe XX (1.2763 – 1.2978 nm), (e) Fe XIX (1.3424 – 1.3520 nm), (f) Fe XVIII (1.6005 – 1.6165 nm), (g) Fe XVII (1.7054 + 1.7097 nm). The vertical dashed lines indicate the peak time of the TESPEL shell ablation for each case. (h) Vertical profile evolution of the Fe XX emissions just before and after the injection of the smaller TESPEL.

In this experiment, the effect of impurity on plasma turbulence was also investigated.

Figure 5 shows the temporal evolution of the frequency spectrum of the n_e fluctuation amplitude for both n_e profile cases with a smaller TESPEL. In all cases, TESPEL injection caused a very transient increase in n_e fluctuations, as measured by the 2D-PCI diagnostic [9]. For the smaller TESPEL into the plasma with the peaked n_e profile, the reduction of the ~20 kHz ne fluctuations lasted only about 0.1 s, and then the characteristics of n_e fluctuations returned to the pre-injection condition. In contrast, for the smaller TESPEL into the plasma with the flat n_e profile, the reduction of the ~20 kHz n_e fluctuations persisted for a much longer period. When considered together with the impurity behaviour, these observations suggest that impurities may be responsible for the reduction in fluctuations, indicating their impact on turbulence.

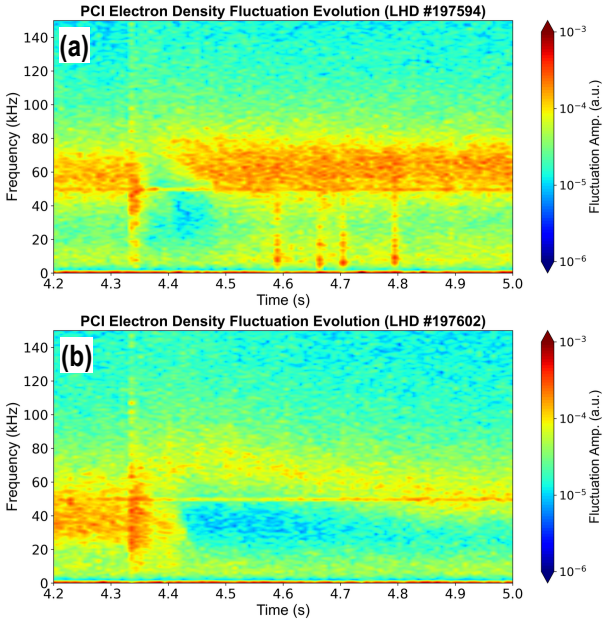

Fig.5. Temporal evolution of the ne fluctuation amplitude frequency spectrum for (a) the plasma with peaked ne profile (LHD #197594) and (b) the plasma with flat ne profile (LHD #197602). The smaller TESPELs were injected in both cases.

Summary The effect of n_e profile shape on Fe impurity behaviour was studied in NBI-heated LHD plasmas using Fe-TESPEL injection. A marked degradation of the core T_e occurred only when the larger TESPEL deposited iron deeply into a plasma with a peaked n_e profile. This case also showed a shift of dominant Fe charge states toward lower charge states as the T_e profile flattened. These observations indicate enhanced impurity accumulation in the core region under this condition. At the same time, the shallow-deposition cases show that impurity behaviour cannot be determined solely from whether the n_e profile is peaked or flat. The line emissions from highly ionized Fe impurities decayed toward its pre-injection level in the peaked n_e case and was shorter-lived than in the flat n_e case. The experiments also revealed distinct low frequency n_e fluctuation responses, suggesting possible coupling between impurity transport, radiation cooling and turbulence. Overall, the impurity deposition location and the background n_e profile both play essential roles in determining impurity confinement in LHD plasmas.

Acknowledgements We would like to thank the LHD experiment group and the technical staff of LHD for their effort to support the experiment in LHD. This work was supported by a NINS Network-type Research Acceleration Program and a JSPS KAKENHI JP23KK0054. This work has been carried out within the framework of the EUROfusion Consortium, funded by the European Union via the Euratom Research and Training Programme (Grant Agreement No. 101052200 - EUROfusion). Views and opinions expressed are those of the authors only and do not necessarily reflect those of the European Union or the European Commission.

References [1] M. Greenwald et al., Phys. Rev. Lett. **53**, 352 (1984)., [2] K. Ida et al., Phys. Rev. Lett. **76**, 1268 (1996). [3] R. Dux et al., J. Nucl. Mater. **313-316**, 1150 (2003). [4] N. Tamura et al., Rev. Sci. Instrum. **92**, 063516 (2021). [5] J.L. Schwob et al., Rev. Sci. Instrum. **58**, 1601 (1987)., [6] M. B. Chowdhuri et al., Appl. Opt. **47**, 135 (2008)., [7]. C. Dong et al., Rev. Sci. Instrum. **81**, 033107 (2010). [8] I. Yamada et al., J. Fusion Energy **44**, 54 (2025)., [9] K. Tanaka et al., Rev. Sci. Instrum. **79**, 10E702 (2008).